Proceedings of the 12th International Conference on the Stability of Ships and Ocean Vehicles, 14-19 June 2015, Glasgow, UK,

1

Potential Assessment of Cargo Fluidization based on an UBC3D-PLM Model

Lei Ju, *Ship Stability Research Centre, University of Strathclyde,* lei.ju@strath.ac.uk

Dracos Vassalos, S*hip Stability Research Centre, University of Strathclyde,* d.vassalos@strath.ac.uk

ABSTRACT

Fluidization of fine particle cargoes, resulting in cargo shift and loss of stability, has caused the loss of many lives in numerous marine casualties over the past decades. Since the dangers of cargo fluidization have long been known to the shipping industry, the question of why the phenomenon is resurfacing now would be a legitimate one. With this in mind, an UBC3D-PLM model based on FEM theory in the commercial software PLAXIS is presented in this paper to consider soil DSS (Direct Simple Shear) test to verify the model. To assess the cargo fluidization potential, an evaluating method is presented in the paper considering cargo fluidization. Shaking table tests with different amplitude, frequency and initial degree of saturation of cargos were studied to predict time-domain characteristics. This method in the paper could be feasibly used as a reference and possibly support a suitable regulatory framework to the fluidization analysis of ship stability.

Keywords: *Cargo Liquefaction; UBC3D-PLM; Ship Stability*

1. INTRODUCTION

Liquefaction of mineral ores, such as ore fines from India and nickel ore from Indonesia, the Philippines and New Caledonia, resulting in cargo shift and loss of stability, has been a major cause of marine casualties over the past few years. Such a transition during ocean carriage can cause a sudden loss of stability of the carrying vessel. While cargoes are loaded on board a vessel, the materiel is exposed to mechanical agitation and energy input in the form of engine vibrations, vessel movement and wave impact, resulting in a gradual settling and compaction of the cargo. The gaps between the particles become smaller in the process, while the pore pressure between particles will increase. The water holding ability or matric suction of particles decreases and the water in the cargos will separate from the cargo. Then cargos turn into a viscous fluid, i.e. fluidization.

The UBC3D-PLM is a powerful constitutive model, which is a 3-D extension of the UBCSAND model introduced by Beaty & Byrne (1998). The Mohr-Coulomb yield condition in a 3-D principal stress space is used. The bulk modulus of water is depended with the degree of saturation, which is specified via PLAXIS input, enabling the prediction of the pore pressure evolution in unsaturated particles.

2. KEY FEATURES OF UBC3D-PLM

2.1 Yield Surface

Mohr-Coulomb yield function generalized in 3-D principal stress space is used in UBC3D-PLM model (Alexandros & Vahid, 2013) as presented in Figure 1.

Proceedings of the 12th International Conference on the Stability of
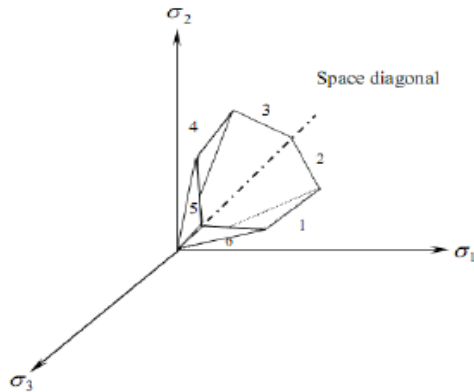Ships and Ocean Vehicles, 14-19 June 2015, Glasgow, UK,

2

Figure 1 The Mohr-Coulomb yield surface in 3-D principal stress space

The critical yield surface could be defined given by Equation (1):

$$f_m = \frac{\sigma'_{max} - \sigma'_{min}}{2} - (\frac{\sigma'_{max} + \sigma'_{min}}{2} + c' \cot \phi'_p) \sin \phi_{mob} \quad (1)$$

Where, σ'_{max} and σ'_{min} are the maximum and minimum principal stresses respectively, c' is the cohesion of the soil, ϕ'_p is the peak friction angle of the soil, ϕ_{mob} is the mobilized friction angle during hardening.

2.2 Elasto-plastic Behaviour

The elastic behaviour which occurs within the yield surface is controlled by two parameters expressed in terms of the elastic bulk modulus K_B^e and the elastic shear modulus K_G^e as shown below:

$$K_B^e = k_B^e P_A \left(\frac{p'}{P_A} \right)^{me} \quad (2)$$

$$K_G^e = k_G^e P_A \left(\frac{p'}{P_A} \right)^{ne} \quad (3)$$

Where, p' is the mean effective stress, P_A is the reference stress (usually equal to 100kPa), k_B^e and k_G^e are the bulk and shear modulus

numbers respectively and, *me* and *ne* are the elastic exponents which define the rate dependency of stiffness.

The hardening rule as reformulated by Tsegaye (2011) in UBC3D-PLM model is given as:

$$d \sin \phi_{mob} = 1.5 K_G^p \left(\frac{p}{P_A} \right)^{np} \frac{P_A}{P_m} \left(1 - \frac{\sin \phi_{mob}}{\sin \phi_{peak}} R_f \right)^2 d\lambda \quad (4)$$

Where, $d\lambda$ is the plastic strain increment multiplier, np is the plastic shear modulus exponent, ϕ_{mob} is the mobilized friction angle, which is defined by the stress ratio, ϕ_{peak} is the peak friction angle and R_F is the failure ratio n_f / n_{ult}, ranging from 0.5 to 1.0.

2.3 Plastic Potential Function

The plastic potential function specifies the direction of the plastic strain. A non-associated flow rule based on the Drucker-Prager plastic potential function is used in the UBC3D-PLM (Tsegaye, 2011). The plastic potential function is formulated as:

$$g = q - a(p' + c \cot \phi_p) \quad (5)$$

$$a = \frac{\sqrt{3} \sin \psi_{mob}}{\cos \theta + \frac{\sin \theta \sin \psi}{\sqrt{3}}} \quad (6)$$

Where, θ equals $30°$ cause the Drucker-Prager surface is fixed in the compression point.

2.4 Post-liquefaction Rule and Cyclic Mobility

From the experimental studies, the stiffness degradation of soil due to the post-liquefaction behaviour of loose non-cohesive soils or due to the cyclic mobility of dense non-cohesive sands is occurred. For modelling this, an

Proceedings of the 12th International Conference on the Stability of
Ships and Ocean Vehicles, 14-19 June 2015, Glasgow, UK,

3

equation is implemented in UBC3D-PLM which gradually decreases the plastic shear modulus as a function of the generated plastic deviatoric strain during dilation of the soil element.

This behaviour is presented in Figure 2 picturing the process of cyclic mobility of dense sand. The stiffness degradation is computed as follows:

$$K_G^p = K_{G,primary}^p * e^{E_{dil}} \qquad (7)$$

$$E_{dil} = \min(110 * \varepsilon_{dil}, fac_{post}) \qquad (8)$$

Where ε_{dil} is accumulation of the plastic deviatoric strain which is generated during dilation of the soil element, the input parameter fac_{post} is the value of the exponential multiplier term.
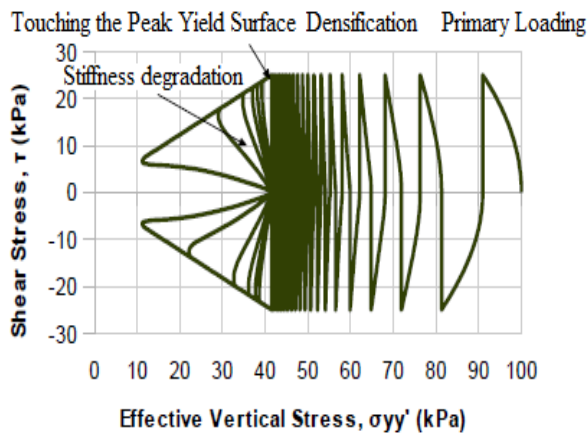
Figure 2   Undrained cyclic shear stress path reproduced with UBC3D-PLM for dense sand. Cyclic mobility, stiffness degradation and soil densification are mentioned on the graph

2.5   Undrained Behaviours

The increment of the pore water pressure is computed by the following equation:

$$dp_w = \frac{K_w}{n} d\varepsilon_v \qquad (9)$$

Where K_w is the bulk modulus of the water and n is the soil porosity and $d\varepsilon_v$ is the volumetric strain of the fluid.

The bulk modulus of water is dependent with the degree of saturation of the soil. The bulk modulus of the unsaturated water is defined as follows:

$$K_w^{unsat} = \frac{K_w^{sat} K_{air}}{SK_{air} + (1-S)K_w^{sat}} \qquad (10)$$

Where K_w^{sat} is the bulk modulus of the saturated water and K_{air} is the bulk modulus of air which equals 1 kPa in this implementation having the minimum value which enables to avoid the generation of pore pressures during modelling a dry sand. S is the degree of saturation in the soil.

3.   VALIDATION OF THE UBC3D-PLM IN ELEMENT TEST

3.1   Validation of the UBC3D-PLM in Monotonic Loading

The validation of the UBC3D-PLM in monotonic loading is presented in this section. The input parameters for modelling the tri-axial compression test (TxC) and the direct simple shear test (DSS) on loose Syncrude sand are given in Table 1. The results of the UBC3D-PLM are in a good agreement with the experimental data (Puebla & Byrne & Philips, 1997) as shown in Figure 3 and Figure 4.

Proceedings of the 12th International Conference on the Stability of
Ships and Ocean Vehicles, 14-19 June 2015, Glasgow, UK,

4

Table 1   UBC3D input parameters for all the validation tests

Parameter	Syncrude S. (TxC, DSS)	Fraser S. (Cyclic DSS)	Cargo (FEM)
$\varphi_p (\circ)$	33.7	33.8	31.2
$\varphi_{cv} (\circ)$	33	33	34.6
k_B^e	300	607	720
k_G^e	300	867	1031
$K_G^p (TxC)$	310	-	
$K_G^p (DSS)$	98.3	266	700
$me = ne$	0.5	0.5	0.5
np	0.5	0.4	0.4
R_f	0.95	0.81	0.74
$N1(60)$	8	8	13
fac_{hard}	1	1	0.45
fac_{post}	0	0.6	0.01

3.2   Validation of the UBC3D-PLM in Cyclic Loading

The behaviour of loose Fraser sand under cyclic direct simple shear is modelled and the numerical results are compared with experimental data as published by Sriskandakumar (2004). The relative density (RD) of the tested sand is 40%. In Figures 5, the evolution of stress-strain is presented. The applied CSR equals 0.08. The vertical applied stress is 100 kPa in all cases. The K0 factor is assumed to be 1 for simplification.
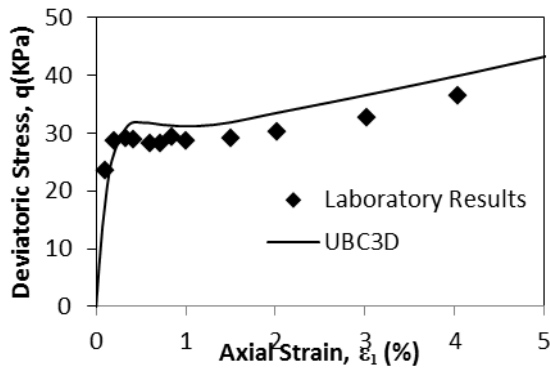
Figure 3 Undrained tri-axial compression
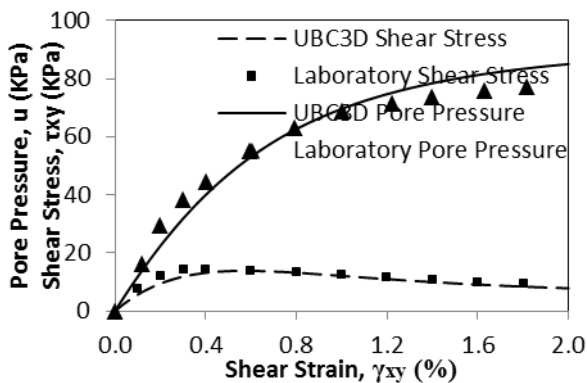
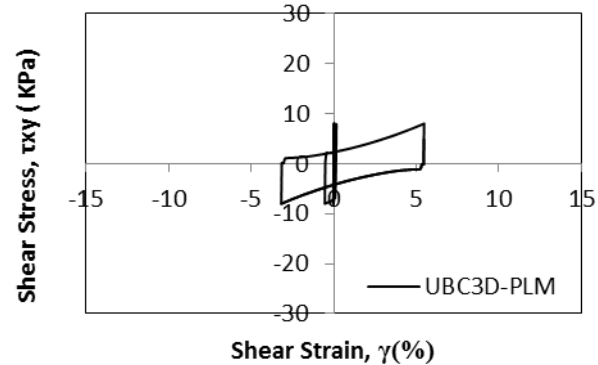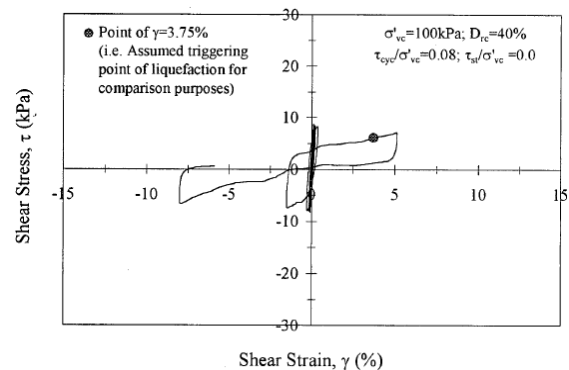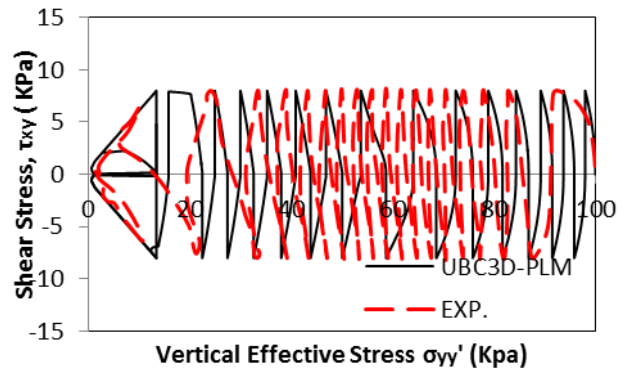
Figure 4   Undrained simple shearing

Figure 5   Cyclic DSS stress controlled (RD=0.4 CSR=0.08 σ_v =100kpa)

Proceedings of the 12th International Conference on the Stability of
Ships and Ocean Vehicles, 14-19 June 2015, Glasgow, UK,

5

4.   CARGO FLUIDIZATION IN A FINITE ELEMENT SCHEME

4.1   Evaluating cargo fluidization

The soil-water characteristic curve is the basis for estimating the dynamic analysis of particles. Unsaturated particles are composed of three phases; including particle skeleton (solid), pore water (liquid) and pore are (gas). The air-water interface has a surface tension. In the unsaturated particles, the pore air pressure and pore water pressure are unequal and greater than the latter. The interface is under the part pore air pressure of lager pore water pressure. The pressure difference (i.e., pore air pressure minus pore water pressure) across the interface of air and water is called the matric suction. Matric suction is generally the key parameter describing the mechanical property of unsaturated particles.

In the capillary tube, the surface between pore air and pore water displays curved interface. The fluid pressure of sides interface is discontinuous. If the upside of the interface is connected with atmosphere, the pressure upside interface is larger than the water pressure. The pressure difference is called matric suction. S depends on the curvature of the curved interface and surface tension.

$$S = u_a - u_w \tag{11}$$

The soil-water characteristic curve (SWCCs) relates the water content or degree of saturation to matrix suction of a particle. A representative SWCCs is shown in Fig 6. We can see different iron ore has different water holding ability. When the cargo compaction, the volume decreases resulting in increasing pore water pressure and decreasing matric suction of cargos. Cargos cannot hold any water in case of suction equals zero. Water is progressively displaced in the hold base, which

may result in some portions or all of the cargo developing a flow state.

For earthquake liquefaction, the acceleration is large and soil could be regarded as un-drained soil, where acceleration for cargo fluidization is small and the water could drain from cargos. When the degree of saturation turns 100% and water comes out from the cargos, the cargos have reflected the nature of fluidization. Therefore, take suction=0 as the onset of cargo fluidization in the paper.
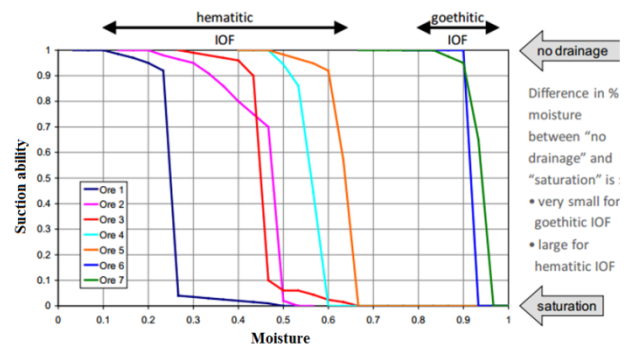
Figure 6 Soil-water characteristic curves

4.2   Centrifuge Test

The influence of degree of saturation on the free field response is investigated. The geometry of layer is shown in Figure 7. Locations L, N, O are monitored through the test. The initial degree of saturation is supposed uniform.
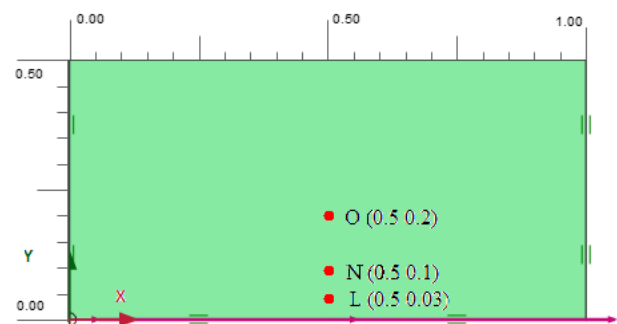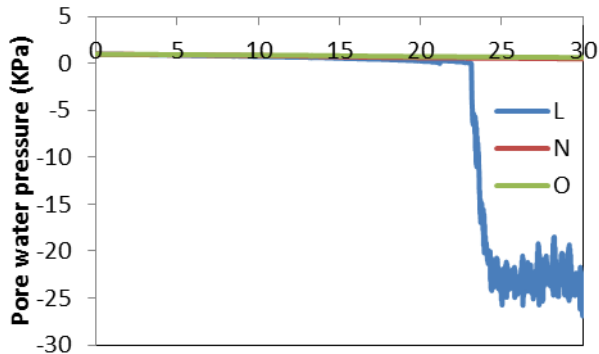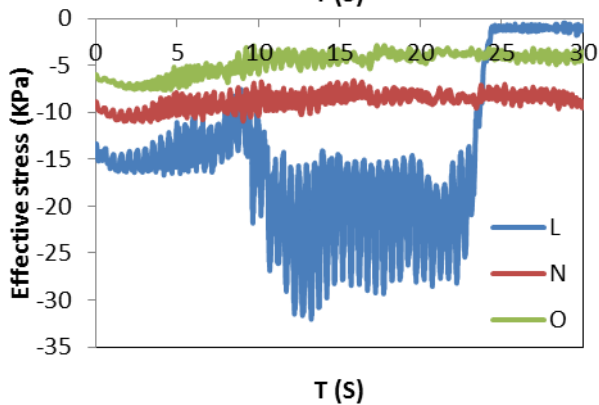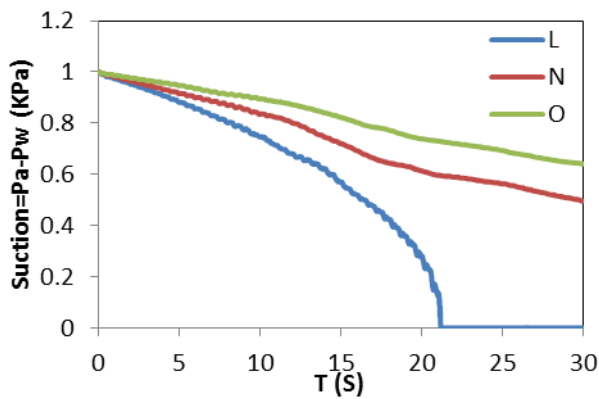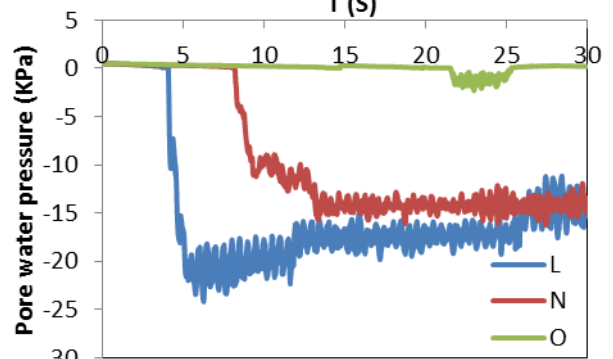
Figure 7   Centrifuge test model

The degree of saturation varies as S=99.0%, 97.0% and 94.0%. The initial stress may have a

Proceedings of the 12th International Conference on the Stability of
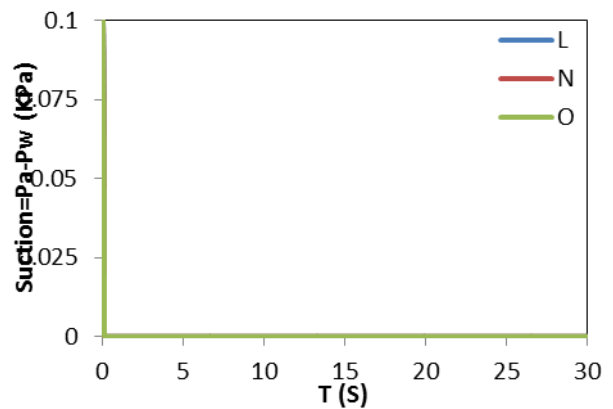Ships and Ocean Vehicles, 14-19 June 2015, Glasgow, UK,

6

great influence on the results and the initial stress used is due to the gravity action during all the tests. The boundary conditions are defined as: at the base of layer, the vertical displacement is blocked, and the input energy is sinusoidal horizontal acceleration with the amplitude $0.02 m/s^2$ and the frequency 2HZ. At the lateral boundaries, the horizontal displacement is blocked. The model parameters are listed in Table 1.
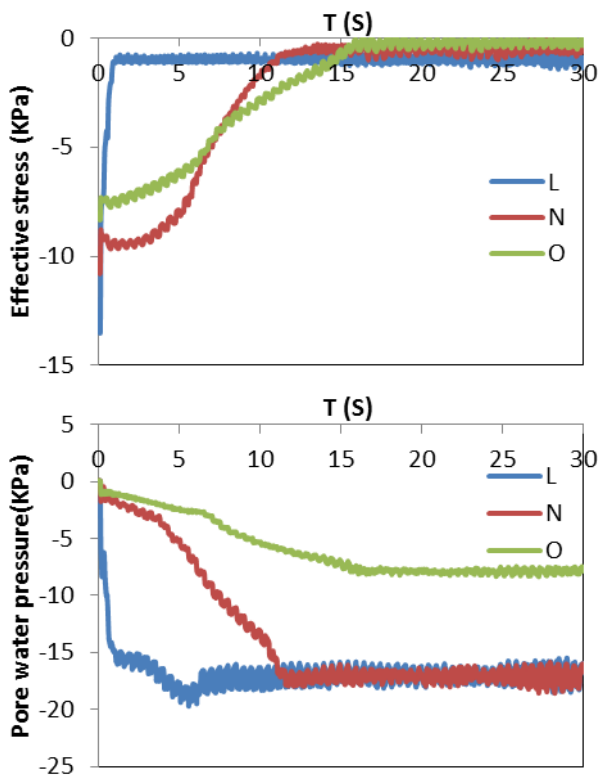
(b) Degree of saturation=97.0%

(a) Degree of saturation=94%

Proceedings of the 12th International Conference on the Stability of Ships and Ocean Vehicles, 14-19 June 2015, Glasgow, UK,

7
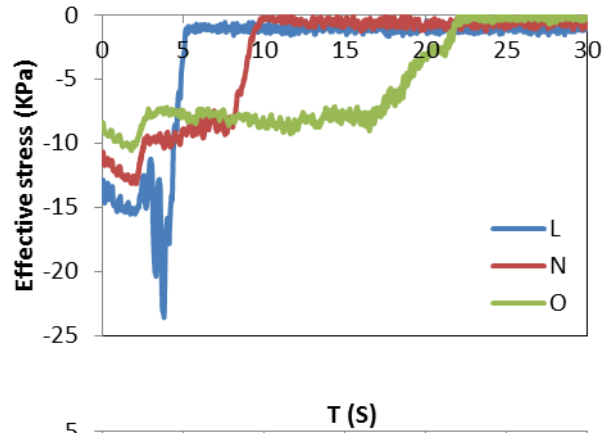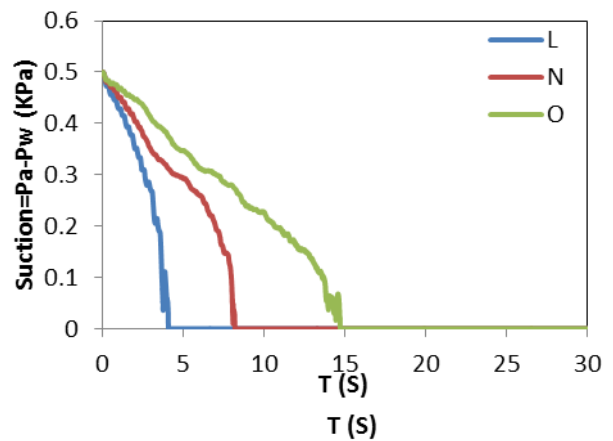
(c) Degree of saturation =99.0%

Figure 8   Evolution of suction, effective stress and pore water pressure of the column during centrifuge test

From Figure 8, we can see that variation of the degree of saturation has a significant influence on matric suction, effective stress and pore water pressure generation. When the matric suction decreases to 0, the degree of saturation turns 100%. From the figure, after full degree of saturation, the pore water pressure increases rapidly and the effective stress decreases to zero and fluidization occurs immediately. when the degree of saturation is less 94%, the onset of fluidization at point L could be delayed to 23s. With the increase in the initial degree of saturation, the onset of fluidization is easier to reach.

4.3   Shaking Table Test

Shaking table tests considering sway motion of ship with different amplitude, frequency and initial degree of saturation of cargos are investigated to predict time-domain

characteristics during liquefaction based on UBC3D-PLM Model in commercial software PLAXIS. The geometry of layer is shown in Figure 9. Locations M, L, K, P, O and N are monitored through the test. The initial degree of saturation is supposed uniform and varies as 99%, 95.16% and 92.38%. The frequency varies as 0.25HZ, 0.35HZ and 0.5HZ. The amplitude varies as 0.02m, 0.04m and 0.06m. The boundary conditions are defined as: rigid box is used in the shaking table test; at the base of layer, the vertical displacement is blocked, and the input energy is sinusoidal horizontal displacement condition. At the lateral boundaries, the horizontal displacement is free and has the same motion with the base of box. The initial stress due to the gravity is shown in Figure 10.
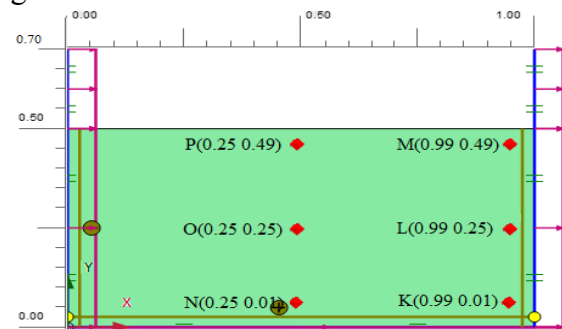

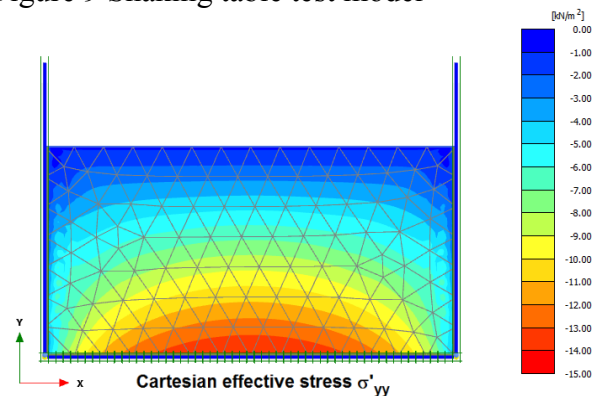Figure 9 Shaking table test model

Figure 10   The effective stress contour after gravity action

From Figure 11 in the calculation of amplitude 0.04m, frequency 0.25HZ and degree of saturation 95.16%, we can see the soil near locations L, O and K is at the edge of liquefaction due to severe contraction. Locations M and P occurs dilation and N has a high effective stress which are difficult to liquefy.
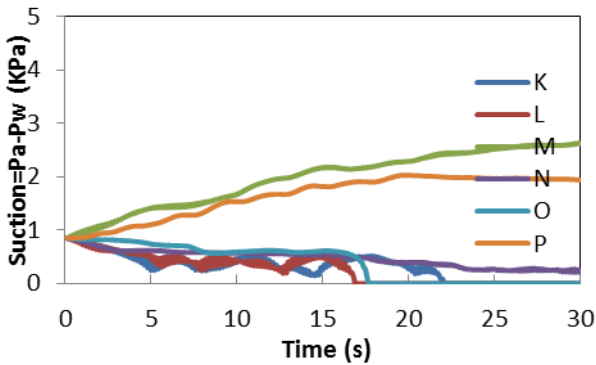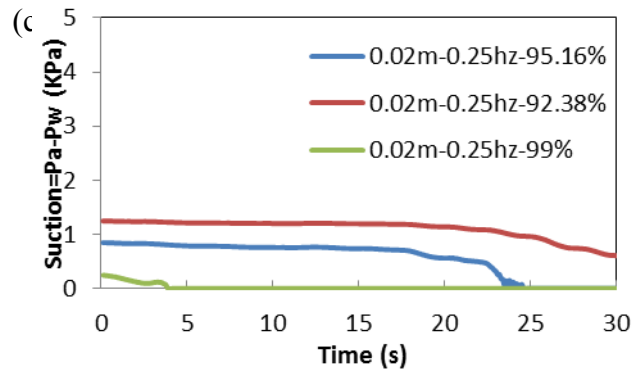
Proceedings of the 12th International Conference on the Stability of
Ships and Ocean Vehicles, 14-19 June 2015, Glasgow, UK,

8

Figure 11   Evolution of suction during shaking table test

(c) Variation with degree of saturation

Figure 12   Evolution of suction at the middle of the column during shaking table test

Emphasis could be put on the middle column of location O. From Figure 12, we can see that the higher degree of saturation, frequency and amplitude, the easier the onset of liquefaction. Due to the interaction between soil and rigid box, liquefaction of the soil displays more complicated from the curves of effective stress. From (a) to (c), varies of the amplitude and the frequency have small impact on liquefaction, where degree of saturation is just the reverse.
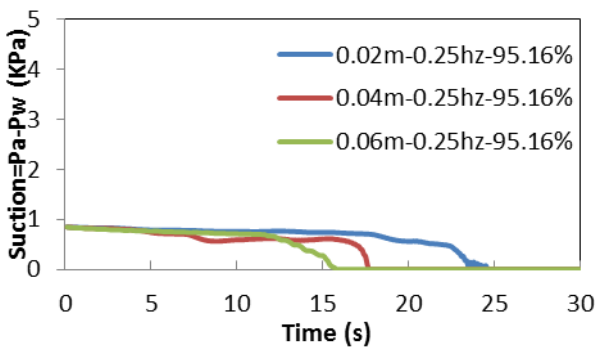

(a) Variation with amplitude

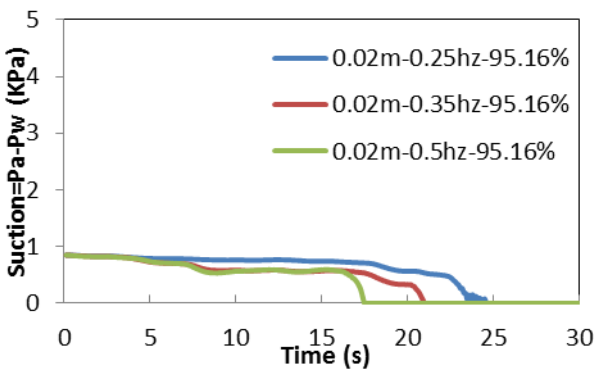(b) Variation with frequency

5.   CONCLUSIONS

Tests for monotonic loading and cyclic loading agree well with experimental data. Finite Element Method combined with UBC3D-PLM model could be used to simulate cargo liquefaction potential assessment. Accurate description for properties of cargos is the key factor to predict cargo liquefaction. In the tests, special properties of soil were used to model the cargo liquefaction.

With the higher degree of saturation, frequency and amplitude, cargo has smaller liquefaction resistance. Among these three factors, the only one we could control is the degree of saturation. Therefore, reducing the degree of saturation of cargos will enormously improve the stability of the cargo ship during transportation.   Comparison with centrifuge test of the single vibration source on the base of column, soil liquefaction with shaking table is more complicated due to the interaction between soil and rigid box.

This method in the paper could be feasibly used as a reference and possibly support a suitable regulatory framework based on time domain analysis of cargo liquefaction.

Proceedings of the 12th International Conference on the Stability of
Ships and Ocean Vehicles, 14-19 June 2015, Glasgow, UK,

9

6. REFERENCES

Beaty, M. and Byrne, P., 1998, "An Effective Stress Model for Predicting Liquefaction Behaviour of Sand", ASCE <u>Geotechnical Earthquake Engineering and Soil Dynamics (geotechnical special publication III)</u>, Vol. 75(1), pp. 766-777.

Petalas, Alexandros. and Galavi, Vahid., 2013, "Plaxis Liquefaction Model UBC3D-PLM", PLAXIS Report.

Puebla, H., Byrne, M., and P.Philips, P., 1997, "Analysis of canlex liquefaction embankments prototype and centrifuge models", <u>Canadian Geotechnical Journal</u>, Vol. 34, pp. 641-651.

Sriskandakumar, S., 2004, "Cyclic loading response of fraser sand for validation of numerical models simulating centrifuge tests", Master's Thesis, The University of British Columbia, Department of Civil Engineering.

Tsegaye, A., 2011, "Plaxis Liquefaction Model", PLAXIS Report.

G.R. Martin, W.D.L. Finn, and H.B. Seed., 1975, "Fundamentals of liquefaction under cyclic loading", Journal of the Geotechnical Engineering Division, ASCE, 101.